JCB Article

Tpr is localized within the nuclear basket of the pore complex and has a role in nuclear protein export

Phyllis Frosst, Tinglu Guan, Cecilia Subauste, Klaus Hahn, and Larry Gerace

Department of Cell Biology, The Scripps Research Institute, La Jolla, CA 92037

Tpr is a coiled-coil protein found near the nucleoplasmic side of the pore complex. Since neither the precise localization of Tpr nor its functions are well defined, we generated antibodies to three regions of Tpr to clarify these issues. Using light and EM immunolocalization, we determined that mammalian Tpr is concentrated within the nuclear basket of the pore complex in a distribution similar to Nup153 and Nup98. Antibody localization together with imaging of GFP-Tpr in living cells revealed that Tpr is in discrete foci inside the nucleus similar to several other nucleoporins but is not present in intranuclear filamentous networks (Zimowska et al., 1997) or in long filaments extending from the pore complex (Cordes et al., 1997) as proposed. Injection of anti-Tpr antibodies into mitotic cells resulted in depletion of Tpr from the nuclear envelope without loss of other pore complex basket proteins. Whereas nuclear import mediated by a basic amino acid signal was unaffected, nuclear export mediated by a leucine-rich signal was retarded significantly. Nuclear injection of anti-Tpr antibodies in interphase cells similarly yielded inhibition of protein export but not import. These results indicate that Tpr is a nucleoporin of the nuclear basket with a role in nuclear protein export.

Introduction

Nuclear pore complexes (NPCs)* are large supramolecular assemblies that provide channels for transport across the nuclear envelope (NE). Although ions, metabolites, and some small proteins (<20–40 kD) can passively diffuse through the NPC, most proteins and RNAs are transported by signal and energy-dependent mechanisms (for reviews see Mattaj and Englmeier, 1998; Gorlich and Kutay, 1999; Nakielny and Dreyfuss, 1999). Most well-characterized signal-dependent transport through the NPC is mediated by nucleocytoplasmic shuttling receptors of the karyopherin or importin/exportin family, which are thought to move through the NPC by interactions with a series of nucleoporins. Importin β by itself or in conjunction with the adaptor importin α is responsible for the import of protein cargoes with basic amino acid–rich nuclear localization signals (NLSs). Crm1, the best characterized protein export receptor, is involved in the export of cargoes with leucine-rich nuclear export signals (NESs). The small GTPase Ran, which directly binds to karyopherins, is thought to play a key role in determining the directionality of nuclear transport (Gorlich and Kutay, 1999).

The NPC has an eightfold radially symmetrical framework that consists of central spokes flanked by nuclear and cytoplasmic rings (for review see Pante and Aebi, 1996). The ring–spoke assembly surrounds an operationally defined gated channel involved in receptor-mediated transport. Eight fibrils extend outward from the cytoplasmic and nucleoplasmic rings. The cytoplasmic fibrils are ∼50-nm long, whereas the nuclear fibrils are ∼100-nm long and often joined at their distal ends by a terminal ring to form a "nuclear basket" (Jarnik and Aebi, 1991; Ris and Malecki, 1993). The cytoplasmic and nuclear fibrils may comprise the initial docking sites for import and export complexes, respectively, before their movement through the central gated channel.

Mammalian NPCs are thought to be composed of up to 50 or more different polypeptides. Several of these have been molecularly characterized and localized to substructures within the pore. These include Nup358 and Nup214 found at the cytoplasmic filaments, Nup98, Nup93, Nup205, Nup153 and Nup50 localized at the nuclear basket, and the Nup62 complex found near the central channel (Stoffler et al., 1999). Many nucleoporins contain multiple copies of the FG (phenylalanine-glycine) dipeptide repeat, and these

The online version of this article contains supplemental material.

Address correspondence to Larry Gerace, 10550 N. Torrey Pines Rd., Imm10, R209, La Jolla, CA 92037. Tel.: (858) 784-8514. Fax: (858) 784-9132. E-mail: lgerace@scripps.edu

*Abbreviations used in this paper: GFP, green fluorescent protein; NE, nuclear envelope; NES, nuclear export signal; NLS, nuclear localization signal; NPC, nuclear pore complex; NRK, normal rat kidney.

Key words: nuclear basket; nuclear foci; nuclear filaments; nuclear transport; nuclear pore complex

FG repeat proteins appear to be interaction sites for karyopherins (for review see Gorlich and Kutay, 1999).

Mammalian Tpr (for translocated promoter region [Mitchell and Cooper, 1992]) is a 265 kD protein associated with the NPC (Byrd et al., 1994). Tpr contains two separate domains: most of the ~1,600 residue NH_2-terminal domain forms a parallel two-stranded coiled-coil interrupted periodically along its length (Hase et al., 2001), which may result in a hinged rod. The remaining ~800 residue COOH-terminal domain is nonhelical and highly enriched in acidic residues. The precise localization of Tpr within the nucleus is controversial. In mammalian cells and *Xenopus* oocytes, Tpr is found near the nucleoplasmic surface of the NPC and is also proposed to be in filaments or hollow cables, which extend up to 350 nm from the nuclear basket into the nuclear interior (Cordes et al., 1997; Fontoura et al., 2001). In cells of the *Drosophila* salivary gland, the Tpr homologue localizes to the nucleoplasmic side of the NE and to extrachromosomal areas within the nucleus (Zimowska et al., 1997) and has been proposed to be a component of an intranuclear filamentous scaffold associated with NPCs (Zimowska et al., 1997; Paddy, 1998).

In *Saccharomyces cerevisiae*, Mlp1p and Mlp2p have predicted secondary structural similarity to Tpr, localize to the nuclear side of the NPC, and are thought to be Tpr homologs (Kolling et al., 1993; Strambio-de-Castillia et al., 1999). A double deletion of *MLP1* and *MLP2* is viable (Strambio-de-Castillia et al., 1999; Kosova et al., 2000) but causes a loss of telomeric clustering (Galy et al., 2000). Moreover, Mlp2p coimmunoprecipitates with Yku70p, a structural component of yeast telomeres (Galy et al., 2000). This suggests a potential role for Mlp1p and Mlp2p in telomere localization. The overexpression of Mlp1p but not Mlp2p results in a nuclear accumulation of poly-$(A)^+$ RNA (Strambio-de-Castillia et al., 1999; Kosova et al., 2000), suggesting a potential role for Mlps in poly-$(A)^+$ RNA export. In mammalian cells, overexpression of full-length Tpr and several Tpr fragments also results in the nuclear accumulation of poly-$(A)^+$ RNA (Bangs et al., 1998). However, because of the long duration of protein overexpression in these experiments it is not clear whether the poly-$(A)^+$ accumulation reflects a direct involvement of Tpr in mRNA export or an indirect effect due to a role of Tpr in another cellular or nuclear transport function.

In this study, we have reevaluated the localization of Tpr in the nucleus using several light microscopy and EM immunolocalization approaches combined with imaging of GFP-tagged Tpr in living cells. We found that Tpr is concentrated at the nucleoplasmic side of the NPC within 120 nm of the pore midplane similar to well-defined nuclear basket proteins. Although we also found Tpr and several other nucleoporins in discrete foci inside the nucleus, we obtained no evidence that it exists in long filaments that are connected to the nuclear basket or that extend through the nuclear interior. Microinjection of anti-Tpr antibodies into mitotic and interphase cells resulted in inhibition of nuclear export of proteins with a leucine-rich NES but did not affect nuclear import of proteins with a basic amino acid–rich NLS. We conclude that Tpr is a nucleoporin that is local-

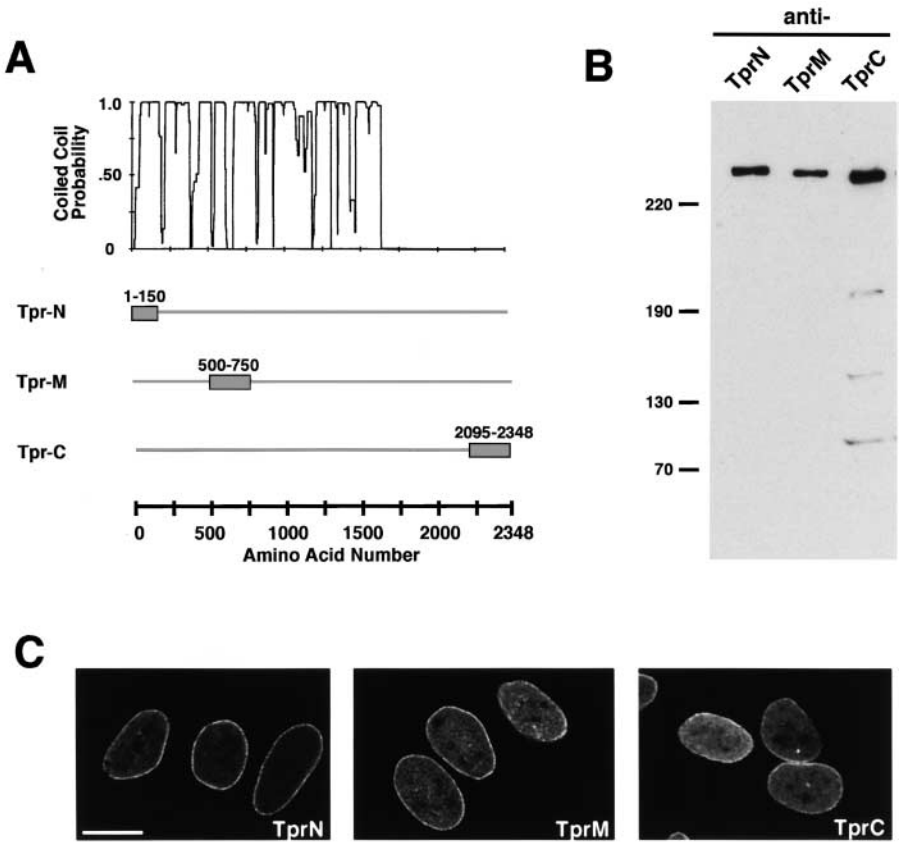

Figure 1. **Characterization of antibodies to three Tpr fragments.** (A) Antibodies against Tpr were made to NH_2- and COOH-terminal fragments and to an internal fragment spanning a break in the predicted coiled-coil region as indicated. (B) HeLa cell extracts were probed by Western blotting with anti-TprN, anti-TprM, and anti-TprC antibodies. (C) HeLa cells were stained with the three anti-Tpr antibodies for immunofluorescence visualization and examined by confocal microscopy. Bar, 5 μm.

ized discretely within the nuclear basket of the NPC and has a role in nuclear protein export.

Results

Localization of Tpr to the NE and discrete foci in the nuclear interior by immunofluorescence microscopy

We have used a combination of immunofluorescence microscopy, light microscope imaging of GFP-Tpr in living cells, and immunogold EM to decisively determine the localization of Tpr. In particular, we wanted to investigate whether Tpr forms long filaments that extend into the nucleus from the NPC and/or a filamentous intranuclear network as proposed (Cordes et al., 1997; Zimowska et al., 1997; Paddy, 1998). Part of the controversy regarding the localization of Tpr may stem from the fact that most previous localization studies used monoclonal or antipeptide antibodies, which have potential problems of cross-reaction with other antigens (Lane and Koprowski, 1982) or limited epitope accessibility. Therefore, we generated affinity purified polyclonal antibodies to 150–250 amino acid fragments from three regions of Tpr in the NH_2 terminus, central region, and COOH terminus (anti-TprN, anti-TprM, and anti-TprC, respectively) (Fig. 1 A). TprN and TprM were located in the NH_2-terminal domain of Tpr, which contains the predicted coiled-coil region, and TprC was located at the end of the COOH-terminal acidic domain (Fig. 1 A). We tested the three affinity purified antibodies for their specificity using immunoblot analysis of HeLa cell extracts (Fig. 1 B). All three antibodies reacted strongly with a single major band that migrated at the position expected for full-length Tpr. Anti-TprC also recognized minor apparent proteolytic fragments in addition to the full-length protein, consistent with the finding that Tpr is extremely sensitive to proteolysis (Byrd et al., 1994; Bangs et al., 1996).

Using our three anti-Tpr antibodies for immunofluorescence staining, we first examined the localization of Tpr in HeLa (Fig. 1 C) and normal rat kidney (NRK) (unpublished data) cells by confocal microscopy. In optical sections through the center of the nucleus, all three antibodies labeled the NE in a punctate pattern characteristic of nucleoporins (Snow et al., 1987) and also yielded staining throughout the nuclear interior as has been observed previously (Bangs et al., 1996; Cordes et al., 1997). The intranuclear Tpr occurred in apparently discrete foci rather than in continuous interconnected zones. In some cells, Tpr was also localized in a diffuse intranuclear pattern and in foci. Immunolocalization of Tpr by confocal microscopy of cul-

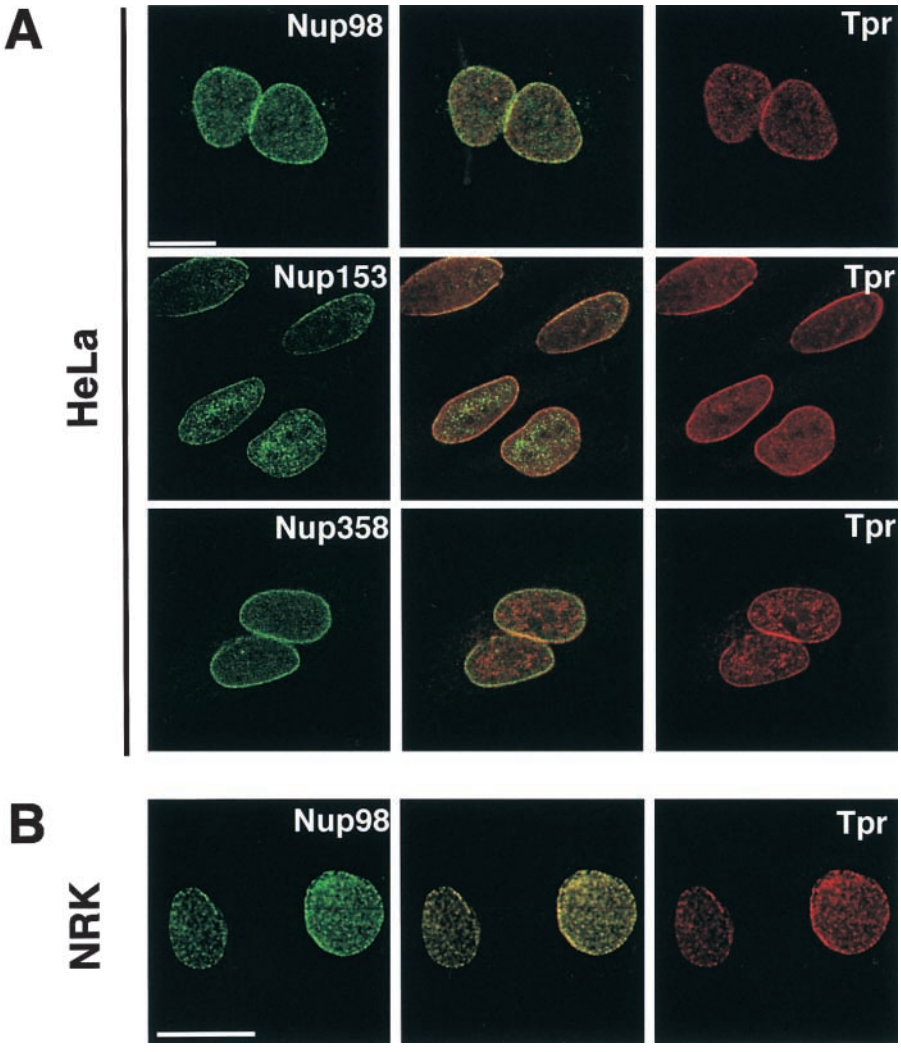

Figure 2. **Localization of Tpr in cultured mammalian cells.** Immunofluorescence staining followed by deconvolution microscopy was used to visualize Tpr (red) in single optical sections HeLa and NRK cells as indicated. Cells are colabeled with antibodies to either Nup98, Nup153, or Nup358 (green). The merged images are shown in the middle. Bars, 5 μm.

tured BRL cells (a rat liver line) and 5 μm cryosections of rat intestine and kidney showed Tpr to be localized at the NE and in discrete intranuclear foci (unpublished data) similar to our findings in HeLa and NRK cells.

We also investigated the localization of Tpr after immunofluorescence staining of cells using deconvolution microscopy. In contrast to confocal microscopy, which removes out-of-focus light from a z-section by optical methods, deconvolution microscopy removes out of focus light using computational methods. Optical sections of HeLa and NRK cells obtained by deconvolution microscopy (Fig. 2) showed that Tpr occurs in a punctate pattern at the NE and in apparently discrete foci throughout the nuclear interior similar to the findings from confocal microscopy. All three anti-Tpr antibodies gave a similar localization pattern by this method. The nuclear basket proteins Nup98 and Nup153 and the cytoplasmic fibril protein Nup358 also were localized at the NE and in intranuclear foci, although these foci largely did not colocalize with the Tpr-containing foci (Fig. 2; unpublished data). Our finding that some Nup98 is present in intranuclear foci is consistent with previous work (Powers et al., 1995; Fontoura et al., 1999), although we do not find extensive colocalization of intranuclear Nup98 and Tpr as reported (Fontoura et al., 2001).

To further investigate whether the intranuclear foci of Tpr we observed in z-sections obtained by deconvolution microscopy are discrete isolated bodies or a two-dimensional cross-sectional view of a three-dimensional network, we constructed volume projections of HeLa cell nuclei from 20 sequential 0.2 μm serial z-sections. In the en-face or edge-on views of the volume projection rotated 90° to each other (Fig. 3 A, left and right, respectively), the intranuclear staining for Tpr shows only discontinuous foci with no evidence of the foci either forming a filamentous intranuclear network or being associated with filaments that emanate from NPCs. This was confirmed by examination of sequential z-sections at 0.4-μm intervals (Fig. 3 B), which shows that individual foci of staining for Tpr (red) and the nuclear basket nucleoporin Nup98 (green) mostly do not overlap, although occasional colocalization of foci is observed. Arrows (Fig. 3 B) indicate foci of Tpr that wax and wane through the sequential sections of the nucleus, showing that foci appear discontinuous. The finding that intranuclear Tpr occurs in discrete intranuclear foci rather than in interconnected net-

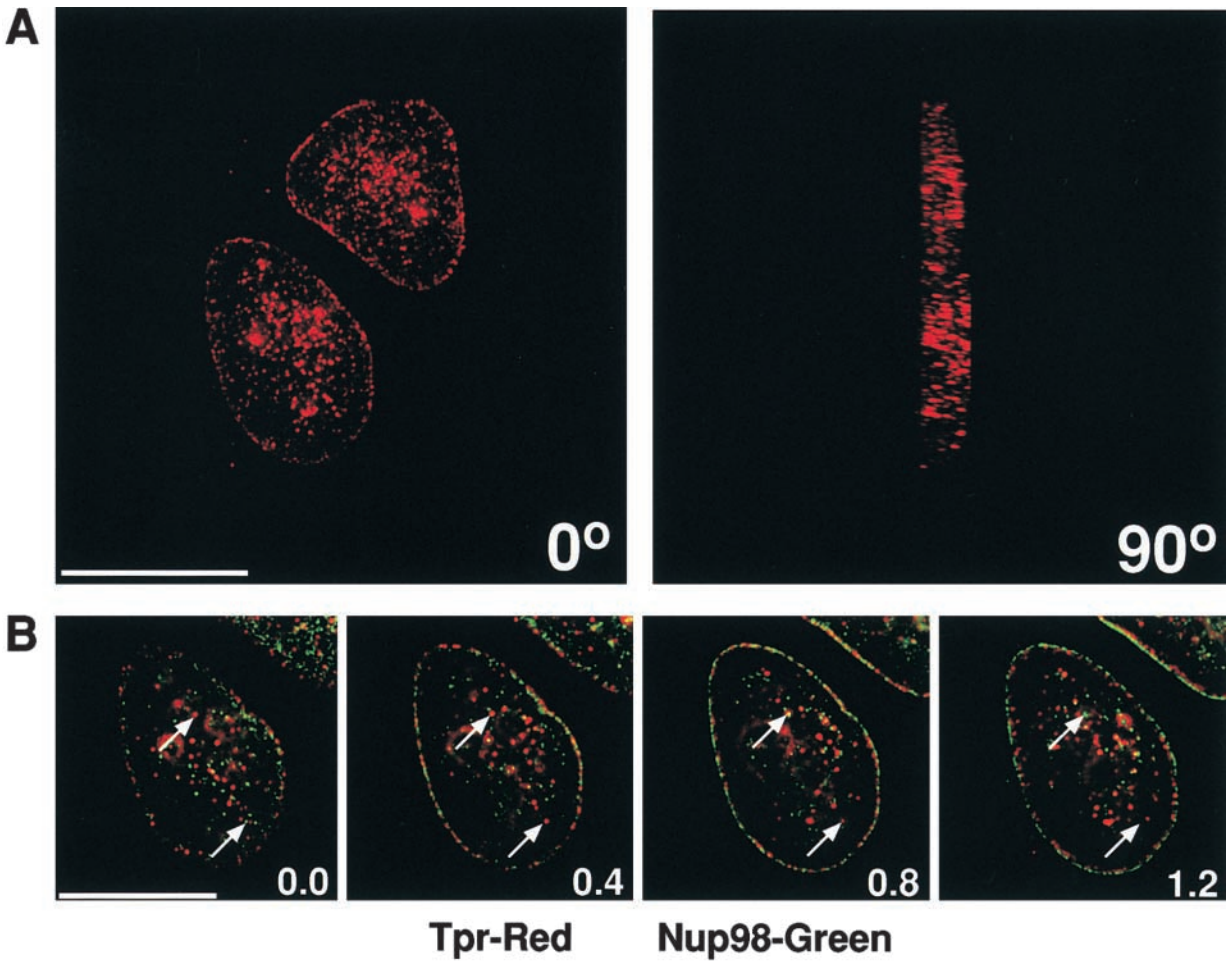

Figure 3. **Localization of Tpr and Nup98 in HeLa cells by immunofluorescence staining and deconvolution microscopy.** (A) Volume projection of 20 sequential 0.2 μm z-sections stained with anti-Tpr antibodies (red). Panels are shown at 0 and 90° to the plane of the slide. (B) Serial z-sections through a nucleus at 0.4-μm intervals. Selected individual foci that successively increase and decrease in intensity are marked by arrows; numbers are in μm. Bars, 5 μm.

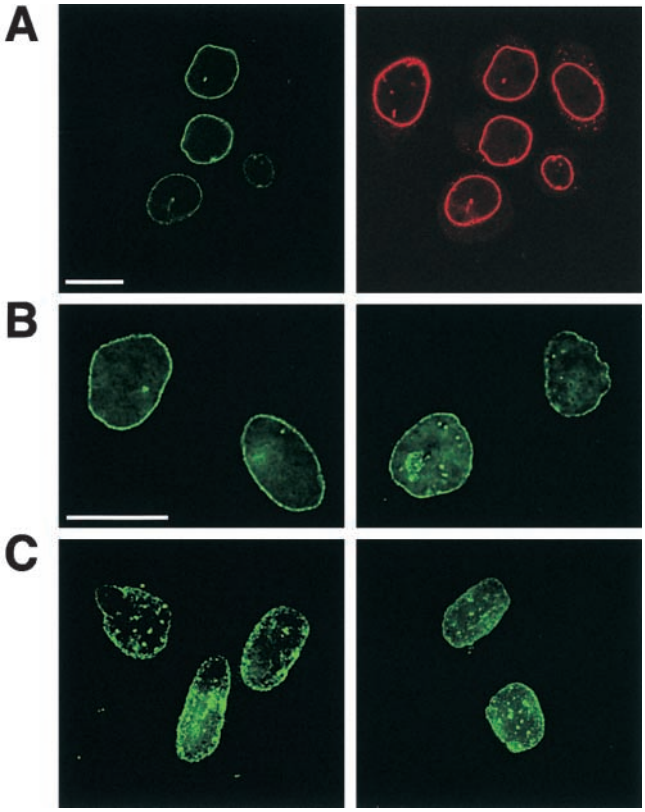

Figure 4. **Imaging of GFP-Tpr in HeLa cells.** Cells were examined 50 h after transfection using confocal (A) or deconvolution (B and C) techniques. (A) Cells were fixed and immunostained with anti-TprC (GFP fluorescence, left, green; anti-TprC, right, red). (B and C) Live cell imaging of GFP-Tpr. Different fields of cells are shown on the left and right. Single optical sections though the middle of the nucleus are shown in A and B; a projected stack of sections encompassing the entire depth of the nuclei is shown in C. See also videos 1 and 2 available at http://www.jcb.org/cgi/content/full/jcb.200106046/DC1. Bars, 5 μm.

works was obtained with several fixation conditions in addition to the standard method used for the images shown (see Materials and methods), which yielded the lowest background. We note that there are differences in the intensities of Tpr and Nup98 in individual foci at the NE (Fig. 3 B). This may reflect different relative concentrations of Tpr and Nup98 in different NPCs.

Imaging of GFP-Tpr in living cells

To verify that our localization of Tpr to discrete intranuclear foci rather than a filamentous network is not an artifact of fixation, we expressed a protein consisting of full-length Tpr tagged with GFP in HeLa cells for live cell imaging. Immunoblot analysis of the transfected cells detected a roughly 300 kD GFP fusion protein as expected (unpublished data). When the transfected cells were fixed and analyzed by immunolabeling and confocal microscopy, the GFP-Tpr (detected by GFP fluorescence) showed a very similar distribution to bulk Tpr (detected by anti-Tpr) in these cells whether low or moderate levels of GFP-Tpr were expressed (Fig. 4 A). Not only was GFP-Tpr efficiently targeted to the NE, but the GFP-Tpr remained stably associated with the NE upon extraction of unfixed cells with PBS containing 0.2% Triton X-100 (unpublished data), suggesting that its interactions with the NE are not grossly perturbed by the GFP tag. Consistent with the fixed cell immunolocalization, imaging of living transfected cells by deconvolution microscopy (Fig. 4, B and C) showed that the GFP-Tpr was localized to both the NE and discrete intranuclear foci and in a diffuse intranuclear pattern (Fig. 4, A and B). The presence of Tpr in foci distributed throughout the nuclear interior can be clearly appreciated in volume projections of stacks of sections (Fig. 4 C). As further evidence that the Tpr localization we obtain by antibody labeling and GFP imaging is very similar, we provide two videos depicting nuclei in which Tpr is localized by antibody staining of untransfected HeLa cells (video 1 available at http://www.jcb.org/cgi/content/full/jcb.200106046/DC1) or by detection of GFP-Tpr in transfected HeLa cells (video 2 available at http://www.jcb.org/cgi/content/full/jcb.200106046/DC1). Both sets of images were generated from a stack of deconvolved optical sections and show the three-dimensional Tpr distribution that can be appreciated by rotating the nucleus. In conclusion, live cell imaging of GFP-Tpr supports the results of antibody localization, showing that intranuclear Tpr is localized diffusely and in discrete foci and is not present in a filamentous intranuclear network.

Localization of Tpr to the nuclear basket of the NPC by immunogold EM

To localize Tpr at high resolution by immunogold EM, we used two complementary techniques: preembedding labeling of cells or isolated nuclei that had been permeabilized to allow antibody access and labeling of ultrathin cryosections of intact cells or tissue in which the entire surface of the section is available for antibody detection. In preembedding analysis of isolated rat liver nuclei (Fig. 5 A) and HeLa cells (Fig. 5, B and C) with anti-Tpr antibodies, we found that strong labeling occurred at the nucleoplasmic side of the NPC as observed previously (Cordes et al., 1997). The labeling occurred within ~120 nm of the pore midplane (Fig. 5, A and C) consistent with a localization to the nuclear basket. It is noteworthy that the strong labeling at the NPC did not continue beyond ~120 nm. Thus, Tpr is unlikely to form filaments or cables that emanate from the nuclear basket into the nuclear interior. In addition to the gold labeling at the NE, single gold particles and small clusters of gold (Fig. 5, asterisks) are also scattered throughout the nucleus. We suggest that the intranuclear clusters of gold labeling reflect the intranuclear Tpr foci observed by light microscopy. In rare cases, clusters of gold particles are seen in the vicinity of an NPC (Fig. 5 A, top asterisk), presumably reflecting the coincidental occurrence of a cluster of intranuclear Tpr near an NPC. We obtained a very similar labeling pattern when we examined ultrathin cryosections of HeLa cells and rat liver by immunogold EM as illustrated by the rat liver samples shown in Fig. 5, D and E. Gold is concentrated at the nuclear surface of the NPC within ~120 nm of the pore midplane and is also found inside the nucleus in clusters and single particles.

A comparison of the distribution of Tpr, Nup153, and Nup98 in the NPC using preembedding immunogold EM of HeLa cells is shown in Fig. 6 where a gallery of high magnification views is presented (left). For all three

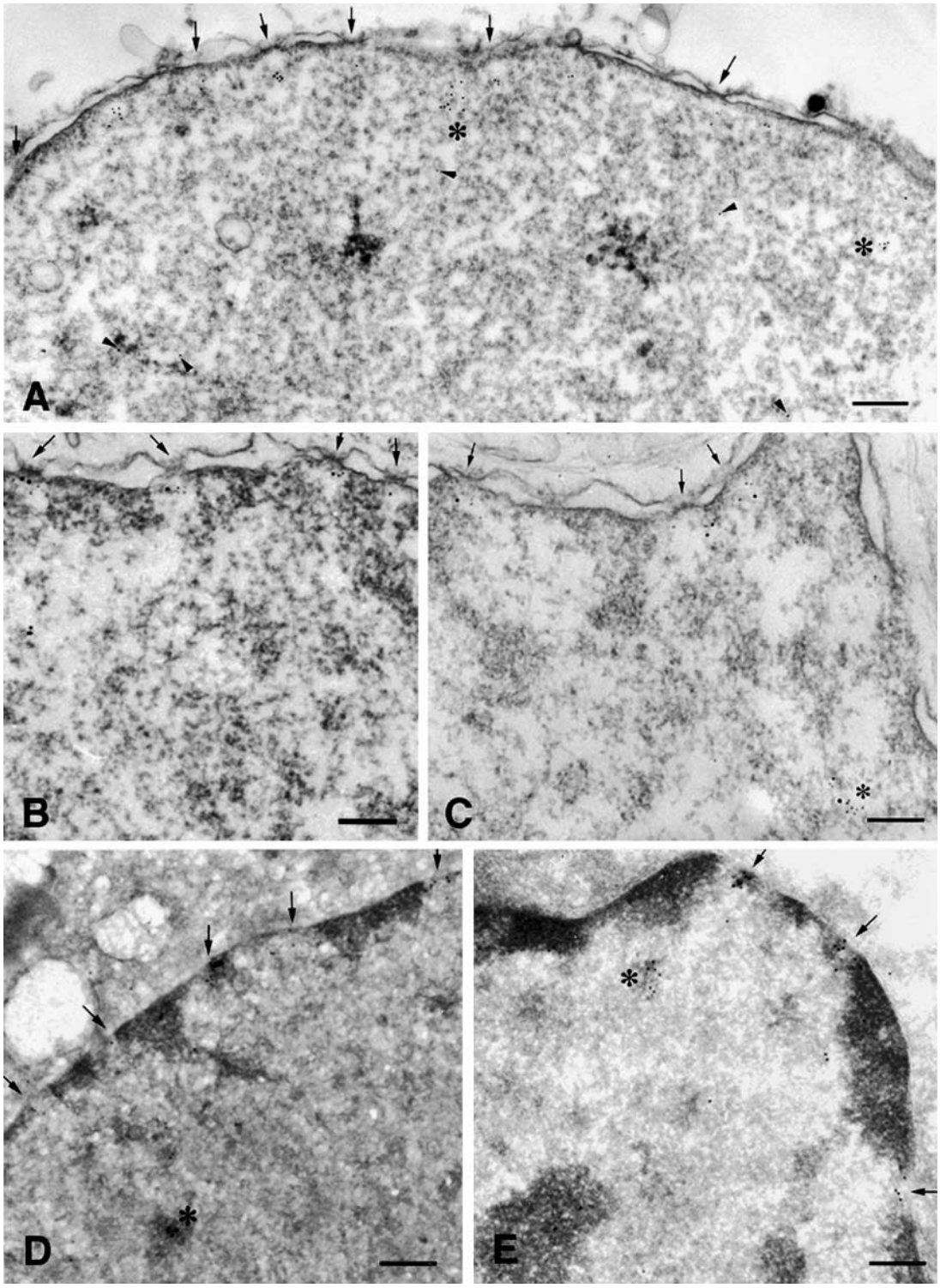

Figure 5. **Immuno-EM localization of Tpr in nuclei of cultured cells and liver.** NPCs are indicated by arrows; gold is seen at the nuclear face of NPCs and also either as single particles (arrowheads) or as clusters in the nuclear interior (asterisks). (A) Tpr was localized by preembedding labeling of rat liver nuclei permeabilized by freeze thawing. (B and C) Tpr was localized by preembedding labeling of HeLa cells, which were permeabilized by freeze thawing. 5-nm gold particles label TprM, and 10-nm gold particles label TprN. (D and E) Tpr was detected by immunogold labeling of ultrathin cryosections of rat liver. Darkly staining matter at the nuclear periphery is condensed chromatin. Bars, 200 nm.

proteins, the NPC-associated gold particles are broadly distributed throughout a zone that is within a ~120 nm radius of the eightfold symmetry axis of the NPC and within a ~120 nm span from the midplane of the NPC (Fig. 6, left). The distribution of gold particles with respect to the midplane of the NPC is quantified in the histograms shown in Fig. 6, A–E (right). The gold particles localizing TprN, TprM, TprC, Nup98, and Nup153 all have broad nucleoplasmic distributions from 20–120 nm of the NPC midplane.

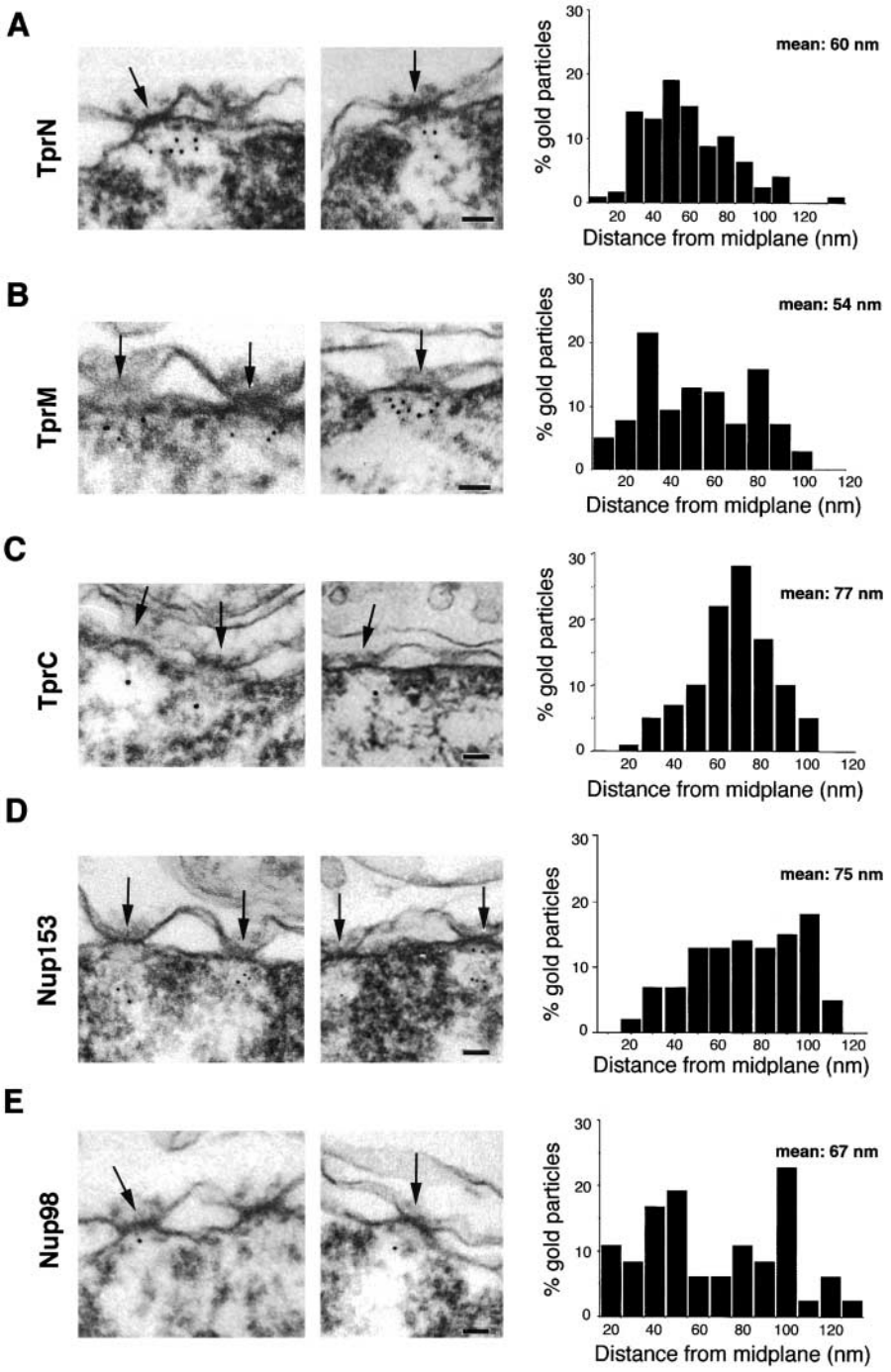

Figure 6. **Immunoelectron microscopic localization of Tpr at the NPC in HeLa cells.** Indirect immunogold labeling was performed for Tpr and the nuclear basket proteins Nup153 and Nup98 in HeLa cells using the preembedding technique. (Left) Gallery of NPCs (arrows) decorated with various antibodies as indicated. (Right) Quantification of gold particle distance from the NPC midplane. (A) anti-TprN, $n = 124$ particles; (B) anti-TprM, $n = 258$ particles; (C) anti-TprC, $n = 105$ particles; (D) anti-TprN and Nup153 $n = 166$ particles for 153; and (E) anti-Nup98, $n = 100$ particles. The average distance from the midplane of the NPC is indicated as mean. Bars, 50 nm.

Table I presents a comparison of the mean distances of gold particles representing Tpr, Nup98, and Nup153 from the midplane of the NPC obtained from analysis of HeLa cells and rat liver by preembedding and cryosectioning techniques. For each of the three antibodies to Tpr, the mean distance from the NPC midplane ranges from 54–77 nm. The mean distance for Nup153 ranges between 75–84 nm, which is further from the NPC midplane than obtained with a monoclonal anti-Nup153 antibody (35–45 nm) presumed to recognize a different epitope (Guan et al., 2000). The mean Nup98 distance is between 53–67 nm, which is also consistent with previously reported results (Radu et al., 1995). Since the distribution of Tpr is very similar to that of the well-recognized nuclear basket components Nup153 and Nup98, this strongly suggests that Tpr is an element of the nuclear basket. The broad distribution of gold particles labeling Tpr on the nucleoplasmic side of the NPC also is consistent with the known flexibility of the nuclear basket, which could result in a variable positioning of epitopes.

Depletion of Tpr from the NE by antibody injection into mitotic cells inhibits nuclear protein export but not import

Until now, the function of Tpr in higher eukaryotes has been studied only by transfection and overexpression of full-length Tpr or fragments of Tpr in cultured cells (Cordes et al.,

Table I. **Distance of Tpr, Nup153, and Nup98 from the midplane of the NPC**

	HeLa		Rat liver nuclei	Rat liver
	Preembedding	Cryosection	Preembedding	Cryosection
		nm		
TprN	60 ± 21 (n = 124)[a,b]	64 ± 29 (n = 152)	67 ± 24 (n = 195)	67 ± 28 (n = 219)
TprM	54 ± 21 (n = 258)	ND	ND	ND
TprC	77 ± 18 (n = 105)	73 ± 29 (n = 160)	68 ± 28 (n = 160)	64 ± 30 (n = 96)
Nup153	75 ± 21 (n = 166)	82 ± 41 (n = 218)	ND	84 ± 42 (n = 189)
Nup98	67 ± 31 (n = 100)	66 ± 41 (n = 157)	ND	53 ± 24 (n = 138)

ND, not determined.
[a]Quantification of gold via immunogold EM.
[b]Numbers in brackets represent the total number of gold particles counted.

1998). However, these studies cannot distinguish whether Tpr overexpression has a direct or indirect effect on nuclear transport, since the phenotypes are determined after the accumulation of overexpressed protein over a 24–48-h period. To more directly examine the role of Tpr in nuclear transport, we used our anti-Tpr antibodies as inhibitory reagents in cell microinjection experiments. This approach has the advantage of being able to examine transport at relatively short time points postinjection. We first investigated whether we could deplete Tpr from the NPC by injecting antibodies into mitotic cells when the NPC is reversibly disassembled.

Mitotic NRK cells (typically in metaphase) were microinjected with a cocktail containing either antibodies against TprN, TprM, or TprC or control IgG and a marker for injection (Alexa fluor 488–conjugated BSA or Alexa fluor 594–conjugated BSA). Injected cells then were incubated at 37°C for up to 4 h during which time they completed mitosis. When the cells were fixed at 4 h and examined by immunofluorescence microscopy, pairs of daughter cells resulting from a single cell that had been injected with anti-Tpr antibodies in the preceding mitosis showed a dramatically reduced level of Tpr compared with that in the adjacent noninjected cells. In contrast, cells injected with control IgG showed Tpr staining similar to that in noninjected cells (Fig. 7). Efficient depletion of Tpr was obtained by injection of either anti-TprN, anti-TprM, or anti-TprC antibodies (Fig. 7; unpublished data). At 1–2 h after antibody injection, Tpr was observed in large aggregates in the nucleus and cytoplasm in most cells (unpublished data), suggesting that the antibody induces the formation of Tpr aggregates, and the aggregated Tpr is subsequently degraded. Sometimes these aggregates persisted at 4 h as seen in the pair of anti-TprC–injected cells in Fig. 7.

When we examined the nuclear basket components Nup153 and Nup98, we found that their staining pattern in cells injected with anti-Tpr antibodies was similar to that in noninjected cells (Fig. 7). Furthermore, immunofluorescence labeling of cells with the monoclonal antibody RL1, which recognizes multiple FG repeat nucleoporins, was indistinguishable in control versus anti-Tpr–injected cells (unpublished data). Taken together, this suggests that other proteins of the NPC, including nuclear basket components, can assemble in the NE at the end of mitosis in the absence of Tpr.

We used this mitotic cell microinjection approach to generate interphase daughter cells with NPCs depleted of Tpr to study the potential role of Tpr in nuclear transport processes. To examine nuclear import, mitotic cells were initially injected with anti-TprN. After 4 h, the resultant daughter cells were then cytoplasmically injected with a fluorescently labeled import cargo containing a basic amino acid–rich NLS (GST-NLS). The level of nuclear import was determined 5 and 30 min after cytoplasmic injection of import cargo. Transport in individual cells was classified by visual inspection of fluorescent images and fell into one of three categories: nuclear fluorescence of import cargo was either greater than the cytoplasmic fluorescence (N > C), equal to the cytoplasmic fluorescence (N = C), or less than the cytoplasmic fluorescence (N < C). At 5 and 30 min after cargo injection, nuclear import in the population of cells that had been mitotically injected with anti-Tpr was not significantly different from import in those cells mitotically injected with control IgG (Fig. 8 and Fig. 9 A), suggesting that Tpr is not essential for this nuclear import pathway.

To examine nuclear protein export, fluorescently labeled export cargo bearing a leucine-rich export signal (GST-NES) was injected into the nucleus of interphase cells that had been injected with anti-Tpr or with control IgG during the preceding mitosis. Export was evaluated at 30 and 60 min after nuclear injection of export cargo. At 30 min after cargo injection, substantial export of the cargo had occurred in most cells that had been injected with control IgG, whereas in cells injected with anti-Tpr antibodies export was significantly impaired (Fig. 8 and Fig. 9 B). The level of export in cells injected with control IgG at mitosis was unchanged at 60 min compared with 30 min. At 60 min in the anti-Tpr–injected cells, the level of export was greater than at 30 min but still had not reached the level of export seen in control cells in only 30 min (Fig. 8 and Fig. 9 B). This indicates that the depletion of Tpr achieved with this approach results in a kinetic impairment of protein export rather than an absolute block.

Microinjection of anti-Tpr antibodies into interphase cells results in the disruption of protein export but not import

As a second approach to address the role of Tpr in nuclear protein transport, we microinjected anti-Tpr antibodies into the nucleus of interphase NRK cells and examined nuclear import and export at short times thereafter. We determined by immunofluorescence staining that there was no apparent

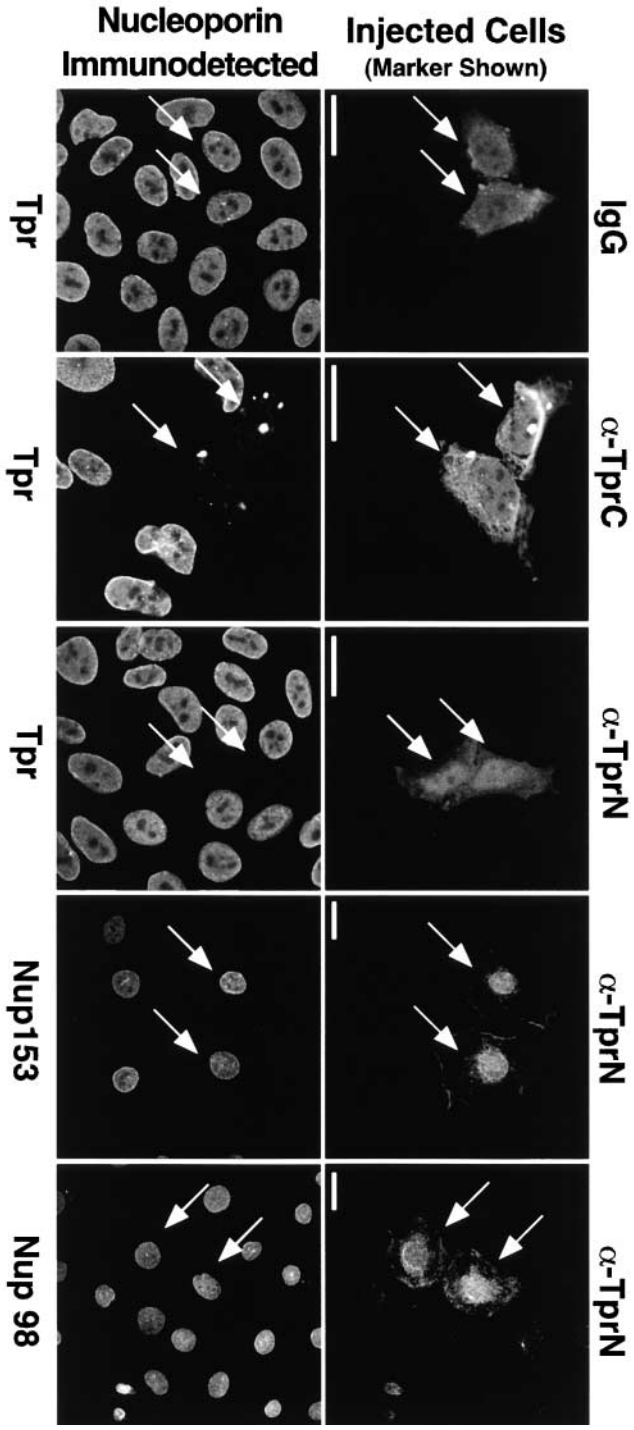

Figure 7. **Immunofluorescent localization of nucleoporins 4 h after microinjection of anti-TprN, anti-TprC, or control rabbit IgG into NRK cells at mitosis.** The injection marker (Alexa fluor 488–conjugated BSA) and rhodamine-coupled secondary antibodies specific to the species in which the injected antibody was raised, which recognize the injected antibodies, identify injected cells (arrows), and are imaged on the right. The labels on the right designate the injected antibody, and the labels on the left indicate which nucleoporin was stained for, using antibodies raised in a different host species and directed against a different segment of Tpr than the injected antibody. The immunodetected nucleoporins are shown on the left. (Guinea pig anti-TprN antibodies and rabbit anti-Nup98 or Nup153 were used for detection, and the complementary species of antibody was used for injection.) Images were acquired by confocal microscopy. Bars, 5 μm.

loss of Tpr from the NE within the time course of these experiments after the nuclear microinjection of antibodies (unpublished data).

To examine protein import, anti-Tpr antibodies (anti-TprN, anti-TprM, or anti-TprC), or control IgG were microinjected into NRK cell nuclei, and import cargo (GST-NLS) was separately microinjected into the cytoplasm at 20–30 min after the initial antibody injection. The GST-NLS import cargo was detected 30 min after its injection by using immunofluorescence microscopy with an antibody to GST. Injected cells were scored for import as above ($N > C$, $N = C$, or $N < C$). We did not observe any significant effect on protein import in cells that had been microinjected with the various anti-Tpr or control (IgG) antibodies (Fig. 10 A).

To examine nuclear protein export, anti-Tpr antibodies or control antibodies were mixed with export cargo (GST-NES), and the cocktail was injected into the nucleus of NRK cells. The level of nuclear export was scored after 30 min as noted above. We observed strong inhibition of export with all three antibodies to Tpr (Fig. 10 B). The distribution of cells among the three nuclear transport categories indicates that there were differences in the relative inhibitory efficacy of different anti-Tpr antibodies with anti-Tpr M having the strongest inhibitory effect and anti-TprC having the weakest effect. However, these differences may reflect the heterogeneity of the different antibody populations (i.e., a variable subpopulation of each antibody may be effective at inhibition). These results are in complete agreement with our microinjection studies in which Tpr was depleted by anti-Tpr injection of mitotic cells. Together, the results strongly suggest a direct role for Tpr in the nuclear export of cargo bearing leucine-rich NES sequences.

Discussion

Localization of Tpr in the nucleus

Previous reports have localized Tpr to the nucleoplasmic side of the NPC (Cordes et al., 1997; Bangs et al., 1998). In addition, Tpr has been proposed to be a scaffolding component of the nucleus, forming long filaments (Cordes et al., 1997) or cables (Fontoura et al., 2001) that extend from the NPC into the nuclear interior or forming an extensive interchromosomal network of filaments (Zimowska et al., 1997). Because of interpretive concerns with the previous studies (see below), we have performed a thorough immunolocalization analysis of endogenous Tpr by light microscopy and EM using polyclonal antibodies directed against three well-spaced 150–250 residue fragments of the protein. We also have imaged GFP-tagged Tpr in living cells.

We obtained a consistent picture of the localization of Tpr in the nucleus with all of our different localization approaches. By EM immunolocalization, we found that Tpr is concentrated at the nuclear basket of the NPC within ~120 nm of the pore midplane similar to the localization of the nuclear basket proteins Nup98 and Nup153. However, we found no evidence for Tpr in filamentous structures that emanate from the NPC into the nuclear interior. To the contrary, we observed that the zone of Tpr concentration at the nuclear side of the NPC abruptly ends outside the con-

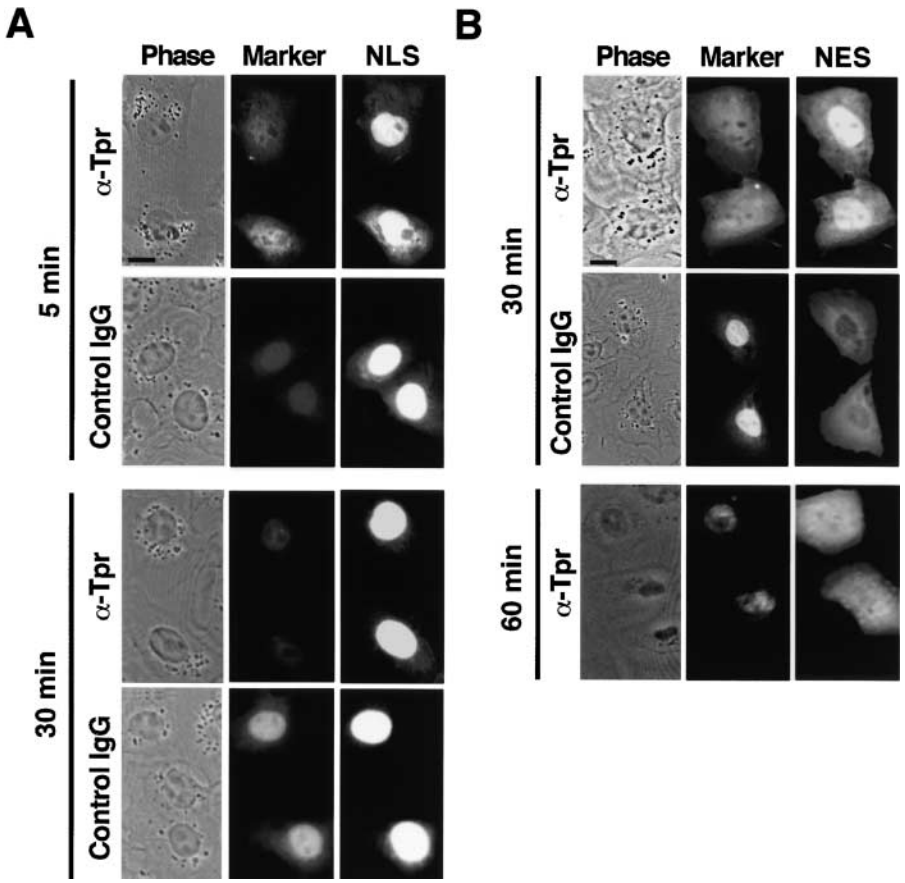

Figure 8. **Analysis of nuclear import and export in NRK cells injected with control IgG or depleted of Tpr by mitotic microinjection of anti-TprN.** (A) Nuclear import of GST-NLS cargo (as described in Materials and methods) 5 and 30 min after cargo injection. The localization of the injection marker (Alexa fluor 488–conjugated BSA) and cargo (NLS) are indicated. (B) Nuclear export of GST-NES at 30 min (for IgG and Tpr) and 60 min (for Tpr only) after cargo injection. Images representative of the three classifications for transport signal are shown: NLS, shows N > C (A, top); NES, shows C > N (B, middle); and NES, shows N = C (B, bottom). Texas red–conjugated BSA was the mitotic cell injection marker used in the 30-min time point for the anti-Tpr injections, and Alexa fluor 488–conjugated BSA was the injection marker used in the 30-min time point for the control IgG injection and the 60-min time point for the anti-Tpr injection. After mitosis, Texas red–conjugated BSA was observed to distribute between the cytoplasm and the nucleus, whereas Alexa fluor–conjugated BSA was observed to segregate to the nucleus. Bars, 5 μm.

fines of the nuclear basket as is the case for other nuclear basket proteins. By all the light microscope localization methods we used, we observed that Tpr is present throughout the nuclear interior and at the NPC. However, the intranuclear Tpr is present in a diffuse localization and discrete foci that are not connected with the NPC and not part of a continuous intranuclear network. We observed that the well-characterized nucleoporins Nup98, Nup153, and Nup358 also are present in discrete intranuclear foci. Thus, the intranuclear localization pattern seen for Tpr is no different from that observed for several other NPC proteins. In conclusion, our results demonstrate that Tpr is a component of the nuclear basket of the NPC and argue that Tpr is not part of filamentous structures that extend into the nuclear interior.

Since the presence of Tpr in intranuclear filaments that emanate from the NPC is widely accepted in the literature (Stoffler et al., 1999; Allen et al., 2000; Ryan and Wente, 2000), it is important to evaluate the discrepancy between our conclusions and those of previous studies. A general concern is that most of the previous localization studies of Tpr have relied on antipeptide or monoclonal antibodies (Cordes et al., 1997; Zimowska et al., 1997; Strambio-de-Castillia et al., 1999; Fontoura et al., 2001), which have much greater potential for cross-reaction (Lane and Koprowski, 1982) or limited epitope accessibility than the antibodies that we generated. Moreover, most previous studies have not simultaneously examined the localization of other nucleoporins in the same sample preparations. This substantially weakens conclusions about a particular localization being specific to Tpr, since it lacks the frame of reference of how other nucleoporins appear under the conditions used. Cordes et al. (1997) used immuno-EM of mammalian tissues and cultured cells to suggest that Tpr is localized to filaments that extend up to 350 nm from the nuclear side of the NPC. However, in these specimens nuclear ultrastructure is poorly preserved, since NEs are swollen and chromatin is detached from the NE, so it is plausible that the fragile nuclear basket is similarly distorted and distended in these preparations. These authors also found that an anti-Tpr antibody labels long filamentous structures extending from the NPC in isolated NEs of *Xenopus* oocytes, but a previous study also found the nuclear basket protein Nup153 in similar filaments (Cordes et al., 1993). Since Nup153 is restricted to the nuclear basket in somatic cells (Pante et al., 1994), this raises the question of whether structures found associated with isolated NEs of oocytes are representative of the somatic cell NE.

In other work, Zimowska et al. (1997) used immunogold EM to examine Tpr in *Drosophila* salivary gland cells and observed concentrated clusters of gold particles outside the chromosomal boundaries. These clusters were suggested to comprise filamentous Tpr (Zimowska et al., 1997). However, whether the Tpr in these interchromosomal spaces is present in filaments or whether it simply represents unassembled intranuclear protein present at a relatively high concentration was not established. An immunogold EM analysis of yeast Mlp1p and Mlp2p showed that they are concentrated at the NE within 120 nm of the pore midplane and are scattered at a lower density throughout the nuclear interior (Strambio-de-Castillia et al., 1999). Although the authors proposed that Mlp1p and Mlp2p form filamentous intranuclear structures that emanate from the NPC, the

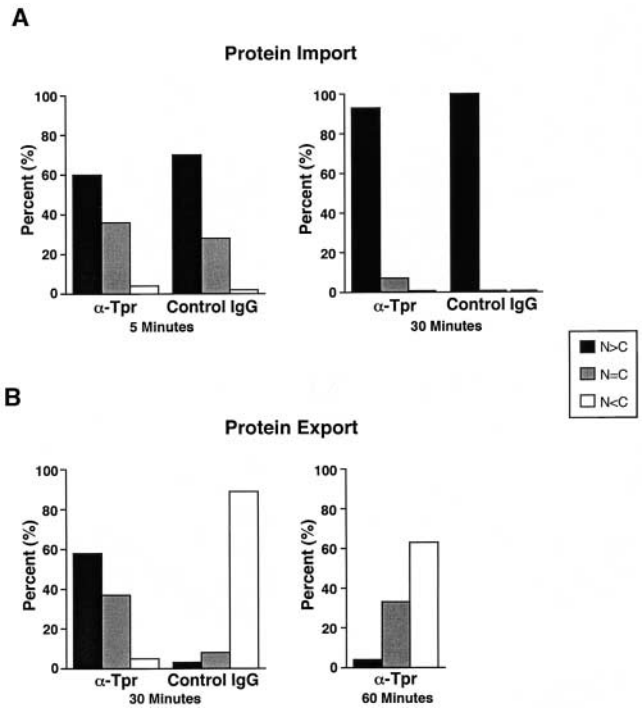

Figure 9. **Analysis of nuclear import and export in interphase NRK cells microinjected with control antibodies or depleted of Tpr by mitotic microinjection of anti-TprN antibodies.** Cells subsequently injected with a fluorescently labeled cargo were fixed at the times indicated and examined by immunofluorescence microscopy. Cells were classified as having nuclear fluorescence greater than (N > C), equal to (N = C), or less than (N < C) cytoplasmic fluorescence. (A) Transport of a basic-type NLS import cargo (GST-NLS) examined at 5 and 30 min after cargo injection. (B) Transport of a leucine-rich NES cargo (GST-NES) at 30 and 60 min after cargo injection in cells injected at mitosis with anti-Tpr antibodies and at 30 min after cargo injection in cells injected at mitosis with control IgG. Between 30 and 50 cells were analyzed for each time point.

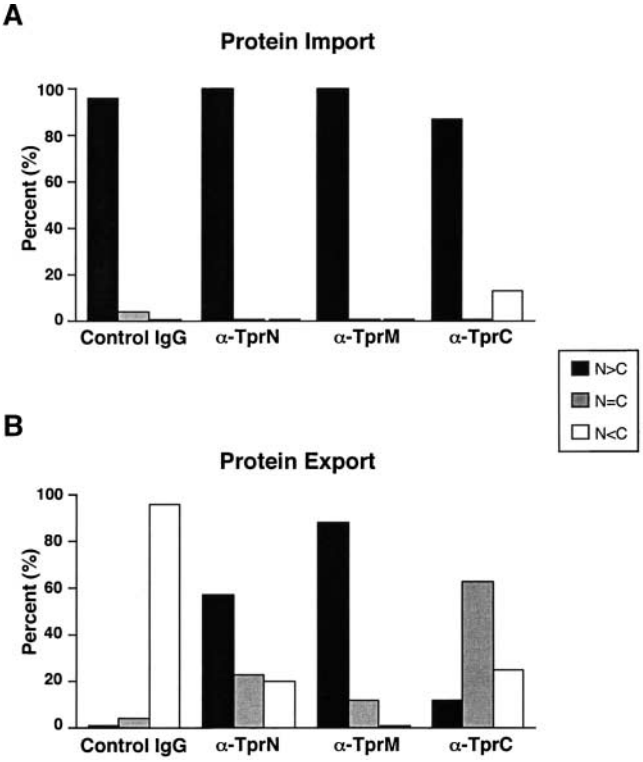

Figure 10. **Analysis of nuclear import and export in interphase cells injected with anti-Tpr or with control IgG antibodies.** Cells were fixed, imaged, and scored for transport as in the legend to Fig. 9. (A) Anti-TprN, anti-TprM, anti-TprC, or control IgG was injected into the nuclei of NRK cells, and after 20–30 min cells were cytoplasmically injected with a basic-type NLS import cargo (GST-NLS). (B) Anti-TprN, anti-TprM, anti-TprC, or control IgG were coinjected into the nuclei of NRK cells with a leucine-rich NES cargo (GST-NES). Between 30 and 50 cells were analyzed for each time point.

distribution of intranuclear Mlp1p and Mlp2p is consistent with the possibility that these proteins occur diffusely or in discrete intranuclear foci rather than in filaments as we have found for mammalian Tpr.

Immunofluorescence microscopy in cultured *Xenopus* cells by Shah et al. (1998) suggested that a COOH-terminal epitope of Tpr was further from the nuclear side of the NE than was an NH_2-terminal epitope of Nup153. This observation was taken to support the model that Tpr comprises NPC-associated filaments. However, since labeling was not performed with antibodies against different Nup153 regions no conclusions can be made on the relative dispositions of Tpr and Nup153 as a whole with respect to the NPC midplane, since the proteins may be in an elongated conformation.

The proposal that Tpr is present in intranuclear filaments has been influenced by the results of scanning EM studies, which have suggested the existence of filamentous structures that underlie the NE or that seem to extend into the nucleus from NPCs (Goldberg and Allen, 1993; Ris and Malecki, 1993; Ris, 1997). The long predicted coiled-coil segment of Tpr and Tpr's localization inside the nucleus make it a tempting candidate to be present in these proposed structures. However, neither Tpr nor any other protein has been identified in these structures by immunolabeling. Moreover, concerns have been raised that many apparent intranuclear filaments may be artifacts of sample preparation (Cook, 1988; Pederson, 2000).

We found that the intranuclear foci of Tpr do not colocalize with foci of other nucleoporins that we have examined, suggesting that they are not part of hypothetical preassembled nuclear basket elements. Nonetheless it is possible that the foci represent nucleoporins synthesized in excess and stockpiled inside the nucleus, awaiting the assembly of new NPCs. In this case, NPC assembly could be regulated by the expression of a small number of limiting (or nucleating) nucleoporins. Alternatively, the foci may represent nucleoporins that dock to and are released from the NPC as part of a transport cycle. Some experiments have suggested that certain nucleoporins can shuttle between the nucleus and the cytoplasm (Boer et al., 1997; Nakielny et al., 1999). However, whether this shuttling occurs on the time scale of nuclear transport is not known.

Functional analysis of Tpr

Our anti-Tpr antibody microinjection experiments provide direct evidence for a role of Tpr in nuclear protein export. In these studies, we used two complementary strategies. First, we depleted Tpr from the nucleus by microinjection of anti-

bodies against Tpr into mitotic cells and assessed the transport competence of the resulting interphase daughter cells. In a complementary approach, we microinjected anti-Tpr antibodies into the nuclei of interphase cells. Both techniques yielded the same result: nuclear import of a cargo containing a basic amino acid–rich NLS proceeded normally, but the rate of nuclear export of a cargo containing a leucine-rich NES was strongly diminished.

The NPC does not appear to be disrupted dramatically when Tpr is depleted by antibody injection into mitotic cells, since the nuclear basket proteins Nup153 and Nup98 and the RL1 antigens showed apparently normal NPC staining, and the cells retained a normal level of nuclear protein import. The ability of NPCs to assemble in the absence of Tpr is consistent with localization studies, which show that Tpr assembles into the NPC later than most nucleoporins at the end of mitosis. (Bodoor et al., 1999; Haraguchi et al., 2000). Together, these results suggest that Tpr is not the backbone of the nuclear basket onto which Nup98 and Nup153 assemble.

Our mitotic cell microinjection analysis cannot exclude the possibility that inhibition of export is due to loss of a hypothetical NPC protein whose assembly into the NPC depends on the presence of Tpr. By contrast, the interphase cell injection experiments do not suffer from this problem, since Tpr remains assembled in the NPC throughout the experiment. In the latter case, the finding that antibodies to three different regions of Tpr inhibited nuclear export but did not affect nuclear import argues that the antibodies are not simply occluding the NPC. Since all phenotypes were scored at relatively short times after antibody injection, we believe that our microinjection approach effectively minimized the interpretive problems associated with previous functional studies, all of which used overexpression of Tpr or fragments thereof (Bangs et al., 1998; Cordes et al., 1998), and involved long time courses such that the observations could reflect indirect effects (as described in Introduction). Considered together, our data strongly argue that Tpr has a direct role in nuclear protein export.

Since Crm1 is the transport receptor for leucine-rich NES cargo used in our injection studies, our results raise the possibility that Tpr may function as an NPC binding site for Crm1 export complexes. In both of our microinjection approaches, we observed a strong decrease in the rate of protein export but not a total block. This may reflect incomplete depletion of Tpr or incomplete obstruction of Tpr with the antibodies. Alternatively, other functionally redundant nucleoporins may compensate for the absence of Tpr. Candidates include the nuclear basket proteins Nup153 and Nup50 both of which bind to Crm1 in a Ran-dependent manner (Nakielny et al., 1999; Guan et al., 2000). It should be noted that Tpr has been observed to coimmunoprecipitate with the import receptor importin β in *Xenopus* oocyte extracts (Shah et al., 1998), and it remains possible that Tpr has a role in some aspect of nuclear import that is not detected by our antibody injection experiments. Our finding that Tpr is a bona fide nucleoporin rather than an NPC-attached intranuclear scaffolding protein provides a new conceptual framework for the analysis of these and other questions.

Materials and methods

Cell culture

Adherent cells (HeLa, normal rat kidney, and Buffalo rat liver [BRL]) were grown in DME, and suspension HeLa cells were grown in S-MEM; both contained 10% FBS and 100 U/ml penicillin and streptomycin.

SDS-PAGE and immunoblotting

Suspension HeLa cells were pelleted at 250 g, resuspended in PBS with protease inhibitors (1 μg/ml aprotinin, pepstatin, leupeptin, AEBSF, E-64, and Bestatin) (Roche Biochemicals), mixed with an equal volume of boiling SDS sample buffer, and incubated at 100°C for 5 min. Protein separation by SDS-PAGE, electrophoretic transfer onto nitrocellulose, and immunoblotting were by standard methods. The Super Signal system (Pierce Chemical Co.) was used for visualization of proteins.

Antibodies

Antibodies were generated against GST fusions to three fragments of human Tpr: residues 1–150 (Tpr N), 500–750 (Tpr M), and 2,095–2,348 (Tpr C). Rabbits and guinea pigs were immunized with the purified fusion proteins, and antibodies were affinity purified as described (Melchior et al., 1995) on a matrix of the purified GST fusion proteins coupled to CNBr-activated Sepharose (Amersham Pharmacia Biotech) at 0.5–1.0 mg/ml. Anti-Tpr antibodies used for interphase cell microinjection experiments were further purified on Trisacryl protein A beads (Pierce Chemical Co.) according to the manufacturer's instructions. For those experiments in which multiple anti-Tpr antibodies were used, all antibodies yielded very similar results. Control rabbit IgG was from Sigma-Aldrich. Antibodies to Nup98 were generated against a 6His-tagged fragment of Nup98 (residues 515–937) and affinity purified. Antibodies against Nup153 (provided by Brian Burke [The Scripps Research Institute, La Jolla, CA] and Iris Ben-Efraim [University of Florida, Gainesville, FL]), lamin A/C, and Nup358 were described in Pante et al. (1994), Schirmer et al. (2001), and Delphin et al. (1997), respectively.

Immunofluorescence microscopy

Cells were grown to ~70% confluency. For standard fixation and permeabilization conditions, cells were fixed in 4% formaldehyde in PBS for 4 min at room temperature, washed with PBS, and permeabilized with 0.2% Triton X-100 in PBS for 4 min. Other conditions tested were fixation of cells with freshly prepared 4% formaldehyde or 4% formaldehyde plus 0.2% glutaraldehyde for 4–20 min followed by permeabilization in 0.2% Triton X-100 for 4–10 min. Alternatively, cells were treated with −20°C methanol for 5 min and −20°C acetone for 5 min, or cells were fixed in 0.2% formaldehyde for 30 min and treated with −20°C acetone for 3 min (Fontoura et al., 1999). These alternate methods resulted in higher background but gave similar results as the standard conditions. After fixation and permeabilization, cells were blocked with 3% BSA, incubated with primary antibodies (0.5 μg/ml) in PBS for 1 h at room temperature, washed with PBS, and incubated for 1 h with Cy5-conjugated goat anti–rabbit or goat anti–guinea pig IgG (1:200; Jackson ImmunoResearch Laboratories) or with FITC-conjugated goat anti–rabbit or goat anti–guinea pig IgG (1:200; Jackson ImmunoResearch Laboratories). The monoclonal antibody RL1 was detected with FITC-conjugated donkey anti–mouse IgM (Jackson ImmunoResearch Laboratories). The specimens were mounted in Slowfade Light mounting medium (Molecular Probes, Inc.) or in Fluoromount G (Electron Microscopy Sciences) and examined with a laser-scanning confocal microscope (model MRC-1024; Bio-Rad Laboratories) or by deconvolution microscopy using a DeltaVision optical sectioning microscope (Model 283; Applied Precision, Inc.). Images were prepared for figures using Canvas 6.0 and Adobe Photoshop® 5.2.

Analysis of GFP-tagged Tpr

The mammalian expression vector containing GFP fused to the COOH terminus of full-length Tpr was generated using pEGFPN1 (CLONTECH Laboratories). Cloning was performed in Stbl2 bacteria (Invitrogen) to prevent recombination events. pGFP-Tpr was transfected into HeLa cells using Fugene 6 (Roche), and live cells were imaged after 48–60 h.

Cell microinjection

For microinjection, cells were grown on glass coverslips 12–24 h before the procedure. Injection cocktails were prepared by combining a single antibody and an injection marker (Alexa fluor 488–conjugated BSA or Alexa fluor 594–conjugated BSA) (Molecular Probes) with or without export cargo (GST-NES) in a 0.5 ml Ultrafree concentrator (Millipore) and adding PBS to a final volume of 0.5 ml. The sample was concentrated 10-fold and

centrifuged at 13,000 *g* for 20 min. Antibodies were injected into mitotic cells at a concentration of 5 mg/ml and into interphase cells at 2 mg/ml. Microinjection experiments used exponentially growing cultures, and metaphase cells were selected by their appearance in phase–contrast microscopy. Cells injected at mitosis were allowed to recover at 37°C for 4 h, and those identified by the fluorescence of the injected marker were microinjected again with either export cargo (a GST fusion to the PKI NES; GST-NES) into the nucleus or with import cargo (a GST fusion to the SV40 T-antigen NLS; GST-NLS) into the cytoplasm. After either 5, 30, or 60 min, cells were fixed in 4% formaldehyde for 5 min and permeabilized with 0.2% Triton X-100 for 4 min at room temperature. Cargo was visualized using a polyclonal goat anti-GST antibody (Amersham Pharmacia Biotech), and an appropriate secondary antibody and cells were examined by fluorescence microscopy. Cells receiving nuclear antibody microinjections at interphase were either coinjected with GST-NES or subsequently cytoplasmically injected 20–30 min after antibody injection with GST-NLS. Graphs were created using Cricket Graph 3 v1.5.3.

Immunogold EM

Immunogold labeling was performed on isolated rat liver nuclei (Dwyer and Blobel, 1976), HeLa, or NRK cells. To permeabilize cultured cells, cells were pelleted in PBS, frozen in liquid nitrogen, and thawed at room temperature. Samples were incubated with anti-TprN, anti-TprM, anti-TprC, anti-Nup98, or anti-Nup153 antibodies (0.5 μg/ml) for 2–3 h at room temperature, washed, and incubated for 2–3 h at room temperature with 5 or 10 nm gold-conjugated anti–rabbit IgG (Sigma-Aldrich) or 12 nm gold-conjugated anti–guinea pig IgG (Jackson ImmunoResearch Laboratories). EM processing was as in Guan et al. (2000).

For cryo-EM, HeLa cells or freshly dissected rat liver were fixed with 4% paraformaldehyde, 0.2% glutaraldehyde, and 4% sucrose in PBS for 1 h at room temperature. Cell pellets and tissues were prepared and sectioned as in Beesley (1993) and Raska et al. (1990). Grids were blocked in 5% FBS for 1 h and then incubated with primary antibodies (0.5 μg/ml) for 1 h. Grids were washed in PBS and blocked in 5% FBS for 30 min and were incubated with secondary antibodies (see above). After washing in PBS for 30–60 min, grids were treated with a mixture of 2% methyl cellulose and 3% uranyl acetate (9:1) and air dried. Micrographs were recorded with a Philips EM-208 at 70–100 kV.

Online supplemental material

Videos 1 and 2 showing three-dimensional rotations of nuclei in which are detected endogenous Tpr and GFP-Tpr (as described in Results) are available at http://www.jcb.org/cgi/content/full/jcb.200106046/DC1.

We gratefully acknowledge the gifts of antibodies from Brian Burke, Iris Ben-Efraim, Christian Delphin, Ralph Kehlenbach, and Eric Schirmer. We thank S. Lyman, S. Sholly, and H. Wodrich for critical reading of this article.

This work was supported by a grant to L. Gerace (GM41955) and K. Hahn (GM57464) from the National Institutes of Health and by a fellowship to P. Frosst from the Fonds pour la Formation de Chercheurs et l'Aide à la Recherche.

Submitted: 8 June 2001
Revised: 21 November 2001
Accepted: 17 December 2001

References

Allen, T.D., J.M. Cronshaw, S. Bagley, E. Kiseleva, and M.W. Goldberg. 2000. The nuclear pore complex: mediator of translocation between nucleus and cytoplasm. *J. Cell Sci.* 113:1651–1659.

Bangs, P.L., C.A. Sparks, P.R. Odgren, and E.G. Fey. 1996. Product of the oncogene-activating gene Tpr is a phosphorylated protein of the nuclear pore complex. *J. Cell. Biochem.* 61:48–60.

Bangs, P., B. Burke, C. Powers, R. Craig, A. Purohit, and S. Doxsey. 1998. Functional analysis of Tpr: identification of nuclear pore complex association and nuclear localization domains and a role in mRNA export. *J. Cell Biol.* 143: 1801–1812.

Beesley, R.C. 1993. Immunocytochemistry: a practical approach. Oxford University Press, Oxford, UK. 266 pp.

Bodoor, K., S. Shaikh, D. Salina, W.H. Raharjo, R. Bastos, M. Lohka, and B. Burke. 1999. Sequential recruitment of NPC proteins to the nuclear periphery at the end of mitosis. *J. Cell Sci.* 112:2253–2264.

Boer, J., J. van Deursen, H. Croes, J. Fransen, and G. Grosveld. 1997. The nucleoporin CAN/Nup214 binds to both the cytoplasmic and the nucleoplasmic sides of the nuclear pore complex in overexpressing cells. *Exp. Cell Res.* 232:182–185.

Byrd, D., D. Sweet, N. Pante, K. Konstantinov, T. Guan, A. Saphire, P. Mitchell, C. Cooper, U. Aebi, and L. Gerace. 1994. Tpr, a large coiled coil protein whose amino terminus is involved in activation of oncogenic kinases, is localized to the cytoplasmic surface of the nuclear pore complex. *J. Cell Biol.* 127:1515–1526.

Cook, P.R. 1988. The nucleoskeleton: artifact, passive framework or active site? *J. Cell Sci.* 90:1–6.

Cordes, V.C., S. Reidenbach, A. Kohler, N. Stuurman, R. van Driel, and W.W. Franke. 1993. Intranuclear filaments containing a nuclear pore complex protein. *J. Cell Biol.* 123:1333–1344.

Cordes, V.C., S. Reidenbach, H.R. Rackwitz, and W.W. Franke. 1997. Identification of protein p270/Tpr as a constitutive component of the nuclear pore complex-attached intranuclear filaments. *J. Cell Biol.* 136:515–529.

Cordes, V.C., M.E. Hase, and L. Muller. 1998. Molecular segments of protein Tpr that confer nuclear targeting and association with the nuclear pore complex. *Exp. Cell Res.* 245:43–56.

Delphin, C., T. Guan, F. Melchior, and L. Gerace. 1997. RanGTP targets p97 to RanBP2, a filamentous protein localized at the cytoplasmic periphery of the nuclear pore complex. *Mol. Biol. Cell.* 8:2379–2390.

Dwyer, N., and G. Blobel. 1976. A modified procedure for the isolation of a pore complex-lamina fraction from rat liver nuclei. *J. Cell Biol.* 70:581–591.

Fontoura, B.M., G. Blobel, and M.J. Matunis. 1999. A conserved biogenesis pathway for nucleoporins: proteolytic processing of a 186-kilodalton precursor generates Nup98 and the novel nucleoporin, Nup96. *J. Cell Biol.* 144:1097–1112.

Fontoura, B.M., S. Dales, G. Blobel, and H. Zhong. 2001. The nucleoporin Nup98 associates with the intranuclear filamentous protein network of TPR. *Proc. Natl. Acad. Sci. USA.* 98:3208–3213.

Galy, V., J.C. Olivo-Marin, H. Scherthan, V. Doye, N. Rascalou, and U. Nehrbass. 2000. Nuclear pore complexes in the organization of silent telomeric chromatin. *Nature.* 403:108–112.

Goldberg, M.W., and T.D. Allen. 1993. The nuclear pore complex: three-dimensional surface structure revealed by field emission, in-lens scanning electron microscopy, with underlying structure uncovered by proteolysis. *J. Cell Sci.* 106:261–274.

Gorlich, D., and U. Kutay. 1999. Transport between the cell nucleus and the cytoplasm. *Annu. Rev. Cell Dev. Biol.* 15:607–660.

Guan, T., R.H. Kehlenbach, E.C. Schirmer, A. Kehlenbach, F. Fan, B.E. Clurman, N. Arnheim, and L. Gerace. 2000. Nup50, a nucleoplasmically oriented nucleoporin with a role in nuclear protein export. *Mol. Cell. Biol.* 20: 5619–5630.

Haraguchi, T., T. Koujin, T. Hayakawa, T. Kaneda, C. Tsutsumi, N. Imamoto, C. Akazawa, J. Sukegawa, Y. Yoneda, and Y. Hiraoka. 2000. Live fluorescence imaging reveals early recruitment of emerin, LBR, RanBP2, and Nup153 to reforming functional nuclear envelopes. *J. Cell Sci.* 113:779–794.

Hase, M.E., N.V. Kuznetsov, and V.C. Cordes. 2001. Amino acid substitutions of coiled-coil protein tpr abrogate anchorage to the nuclear pore complex but not parallel, in-register homodimerization. *Mol. Biol. Cell.* 12:2433–2452.

Jarnik, M., and U. Aebi. 1991. Toward a more complete 3-D structure of the nuclear pore complex. *J. Struct. Biol.* 107:291–308.

Kolling, R., T. Nguyen, E.Y. Chen, and D. Botstein. 1993. A new yeast gene with a myosin-like heptad repeat structure. *Mol. Gen. Genet.* 237:359–369.

Kosova, B., N. Pante, C. Rollenhagen, A. Podtelejnikov, M. Mann, U. Aebi, and E. Hurt. 2000. Mlp2p, a component of nuclear pore attached intranuclear filaments, associates with nic96p. *J. Biol. Chem.* 275:343–350.

Lane, D., and H. Koprowski. 1982. Molecular recognition and the future of monoclonal antibodies. *Nature.* 296:200–202.

Mattaj, I.W., and L. Englmeier. 1998. Nucleocytoplasmic transport: the soluble phase. *Annu. Rev. Biochem.* 67:265–306.

Melchior, F., T. Guan, N. Yokoyama, T. Nishimoto, and L. Gerace. 1995. GTP hydrolysis by Ran occurs at the nuclear pore complex in an early step of protein import. *J. Cell Biol.* 131:571–581.

Mitchell, P.J., and C.S. Cooper. 1992. The human tpr gene encodes a protein of 2094 amino acids that has extensive coiled-coil regions and an acidic C-terminal domain. *Oncogene.* 7:2329–2333.

Nakielny, S., and G. Dreyfuss. 1999. Transport of proteins and RNAs in and out of the nucleus. *Cell.* 99:677–690.

Nakielny, S., S. Shaikh, B. Burke, and G. Dreyfuss. 1999. Nup153 is an M9-con-

taining mobile nucleoporin with a novel Ran-binding domain. *EMBO J.* 18: 1982–1995.

Paddy, M.R. 1998. The Tpr protein: linking structure and function in the nuclear interior? *Am. J. Hum. Genet.* 63:305–310.

Pante, N., and U. Aebi. 1996. Molecular dissection of the nuclear pore complex. *Crit. Rev. Biochem. Mol. Biol.* 31:153–199.

Pante, N., R. Bastos, I. McMorrow, B. Burke, and U. Aebi. 1994. Interactions and three-dimensional localization of a group of nuclear pore complex proteins. *J. Cell Biol.* 126:603–617.

Pederson, T. 2000. Half a century of "the nuclear matrix". *Mol. Biol. Cell.* 11:799–805.

Powers, M.A., C. Macaulay, F.R. Masiarz, and D.J. Forbes. 1995. Reconstituted nuclei depleted of a vertebrate GLFG nuclear pore protein, p97, import but are defective in nuclear growth and replication. *J. Cell Biol.* 128:721–736.

Radu, A., M.S. Moore, and G. Blobel. 1995. The peptide repeat domain of nucleoporin Nup98 functions as a docking site in transport across the nuclear pore complex. *Cell.* 81:215–222.

Raska, I., R.L. Ochs, and L. Salamin-Michel. 1990. Immunocytochemistry of the cell nucleus. *Electron Microsc. Rev.* 3:301–353.

Ris, H. 1997. High-resolution field-emission scanning electron microscopy of nuclear pore complex. *Scanning.* 19:368–375.

Ris, H., and M. Malecki. 1993. High-resolution field emission scanning electron microscope imaging of internal cell structures after Epon extraction from sections: a new approach to correlative ultrastructural and immunocytochemical studies. *J. Struct. Biol.* 111:148–157.

Ryan, K.J., and S.R. Wente. 2000. The nuclear pore complex: a protein machine bridging the nucleus and cytoplasm. *Curr. Opin. Cell Biol.* 12:361–371.

Schirmer, E.C., T. Guan, and L. Gerace. 2001. Involvement of the lamin rod domain in heterotypic lamin interactions important for nuclear organization. *J. Cell Biol.* 153:479–490.

Shah, S., S. Tugendreich, and D. Forbes. 1998. Major binding sites for the nuclear import receptor are the internal nucleoporin Nup153 and the adjacent nuclear filament protein Tpr. *J. Cell Biol.* 141:31–49.

Snow, C.M., A. Senior, and L. Gerace. 1987. Monoclonal antibodies identify a group of nuclear pore complex glycoproteins. *J. Cell Biol.* 104:1143–1156.

Stoffler, D., B. Fahrenkrog, and U. Aebi. 1999. The nuclear pore complex: from molecular architecture to functional dynamics. *Curr. Opin. Cell Biol.* 11: 391–401.

Strambio-de-Castillia, C., G. Blobel, and M.P. Rout. 1999. Proteins connecting the nuclear pore complex with the nuclear interior. *J. Cell Biol.* 144:839–855.

Zimowska, G., J.P. Aris, and M.R. Paddy. 1997. A *Drosophila* Tpr protein homolog is localized both in the extrachromosomal channel network and to nuclear pore complexes. *J. Cell Sci.* 110:927–944.